

Radio-frequency-dressed atoms beyond the rotating wave approximation

S. Hofferberth,^{1,*} B. Fischer,¹ T. Schumm,² J. Schmiedmayer,^{1,2} and I. Lesanovsky^{1,3,†}

*¹Physikalisches Institut, Universität Heidelberg,
Philosophenweg 12, D-69120 Heidelberg, Germany*

*²Atominstitut der Österreichischen Universitäten,
TU-Wien, Stadionallee 2, A-1020 Vienna, Austria*

*³Institute of Electronic Structure and Laser,
Foundation for Research and Technology - Hellas,
P.O. Box 1527, GR-71110 Heraklion, Greece*

(Dated: March 22, 2019)

Abstract

We study atoms dressed with a strong radio-frequency field in a regime where the rotating wave approximation (RWA) breaks down. We present a full calculation of the atom - field coupling which shows that the non-RWA contributions quantitatively alter the shape of the emerging dressed adiabatic potentials. Furthermore they lead to additional allowed transitions between dressed levels. We use RF spectroscopy of Bose-Einstein condensates trapped in the dressed state potentials to directly observe the transition from the RWA to the beyond-RWA regime.

PACS numbers: 03.75.Be, 32.80.Pj, 42.50.Vk

Using external oscillating fields in order to manipulate atoms is a well-established experimental technique. Quantum optics provides a description of such driven atoms in terms of dressed states [1]. These new eigenstates contain contributions from both the atom and the external (dressing) field. Consequently the atomic properties are altered with respect to the field free case. This gives rise to effects like the Autler-Townes [2] splitting or electromagnetically induced transparency [3, 4]. Moreover, the resulting atomic level shift can be utilized for manipulating the external degrees of freedom. In the optical regime the corresponding light shift is used to build traps by exploiting spatial intensity modulation of standing light waves [5]. In the radio-frequency (RF) domain the dressing of Zeeman states has recently been successfully employed to build complex traps and interferometers [6, 7, 8].

A common approximation which is generally used in the context of dressed states is the rotating wave approximation (RWA), where during the derivation of the equations of motion of the dressed system, rapidly oscillating terms are neglected [1]. This approximation is valid if the frequency ω of the driving field is near-resonant with the coupled atomic transition ω_0 , i.e $\omega \approx \omega_0$, and the Rabi frequency of the driving field $\Omega_R \ll \omega$ is much smaller than its oscillation frequency [9].

In this letter, we show that in atom chip RF-traps both conditions for the validity of the RWA can be violated, i.e. locally detunings $\Delta = \omega - \omega_0$ and Rabi frequencies Ω_R become comparable to the driving frequency ω . We use RF spectroscopy [10] to investigate the dressed states and compare our data to the RWA calculation and to a numerically exact calculation in a second quantization picture. We find significant quantitative deviations from the RWA for the resulting adiabatic potentials.

In RF dressing of atoms the coupled states are the Zeeman-shifted magnetic sublevels of an atomic hyperfine state [11, 12]. We denote the static magnetic field causing the Zeeman shift by $\mathbf{B}_S(\mathbf{r})$. The atomic states are coupled by an oscillating magnetic field $\mathbf{B}_{\text{RF}}(\mathbf{r})e^{i\omega_{\text{RF}}t}$. The total Hamiltonian then reads

$$\begin{aligned}
H = & \mu|\mathbf{B}_S(\mathbf{r})|F_z + \hbar\omega_{\text{RF}}a^\dagger a + \gamma [B_{\text{RF}\perp}(\mathbf{r})a^\dagger + \text{h.c.}] F_x \\
& + \gamma [B_{\text{RF}\parallel}(\mathbf{r})a^\dagger + \text{h.c.}] F_z,
\end{aligned} \tag{1}$$

with $\mu = \mu_B g_F$ and $\gamma = \mu/(2\sqrt{\langle N \rangle})$, where μ_B is Bohr's magneton and g_F is the Landé-factor of the considered hyperfine state. $\langle N \rangle$ is the average photon number of the dressing field, \mathbf{F} is the operator of the total atomic spin, and $B_{\text{RF}\perp}(\mathbf{r})$, $B_{\text{RF}\parallel}(\mathbf{r})$ are the complex

amplitudes of the RF field components perpendicular and parallel to the static field vector. a^\dagger is the creation operator for quanta of the RF field.

The first term of the Hamiltonian describes the Zeeman shift of the atomic levels in the static field, while the second term accounts for the energy of the RF field. The coupling between the atomic levels and the dressing field is established by the third and the fourth term. The latter involves only components of $\mathbf{B}_{\text{RF}}(\mathbf{r})$ that oscillate parallel to the static field and can be neglected if $|\mu\mathbf{B}_{\text{RF}\parallel}(\mathbf{r})| \ll \hbar\omega$ [13].

In order to study the non-RWA effects we diagonalize the full Hamiltonian (1) numerically for $F = 2$ in the basis spanned by the bare states $\{|m_F, \Delta N\rangle\}$, where m_F is the magnetic quantum number of the atomic level and $\Delta N = N - \langle N \rangle$, with N being the number of RF photons. The RF field is best described by a coherent state, i.e. a superposition of number states with a poissonian distribution around $\langle N \rangle$. We are not interested in the change of the RF field during the coupling and assume $\langle N \rangle$ to be large. Therefore we only consider a small number of photon states centered around the mean photon number [14].

It is convenient to group these states into manifolds $\{|m_F, \kappa \times F - \text{sgn}(g_F) m_F\rangle\}$, ($m_F = -F, \dots, F$) which are denoted by the number κ . How many manifolds are required for the calculation depends on the strength of the off-resonant contributions to the coupling term in Hamiltonian (1), which introduce a coupling between manifolds with $|\kappa - \kappa'| = 2$. In the numeric calculations we include 25 manifolds ($\Delta N = -12, \dots, 12$) to avoid numerical artifacts.

Considering only a single κ -manifold of bare states in the diagonalization is equivalent to applying the RWA, in which case the resulting potentials take on the well known form [12]

$$V_{\text{RWA}}(\mathbf{r}) = \tilde{m}_F \text{sgn}(\mu) \sqrt{\Delta^2(\mathbf{r}) + \Omega^2(\mathbf{r})} \quad (2)$$

with the detuning $\Delta(\mathbf{r}) = |\mu||\mathbf{B}_S(\mathbf{r})| - \hbar\omega$ and the Rabi frequency $\Omega(\mathbf{r}) = \frac{\mu}{2}|B_{\text{RF}\perp}(\mathbf{r})|$. In this case, the resulting dressed states can be grouped in manifolds $|\tilde{m}_F, (\kappa)\rangle$, where $\tilde{m}_F = -F, \dots, F$ is the effective magnetic quantum number of the dressed states. These manifolds can be characterized by a single κ , because in the RWA case each dressed state only contains contributions of bare states from one κ manifold.

This is no longer true if the off-resonant terms become significant. Then each dressed state becomes a superposition of bare states from many manifolds. Still, for the coupling strengths considered here, it remains possible to identify groups of five dressed states each,

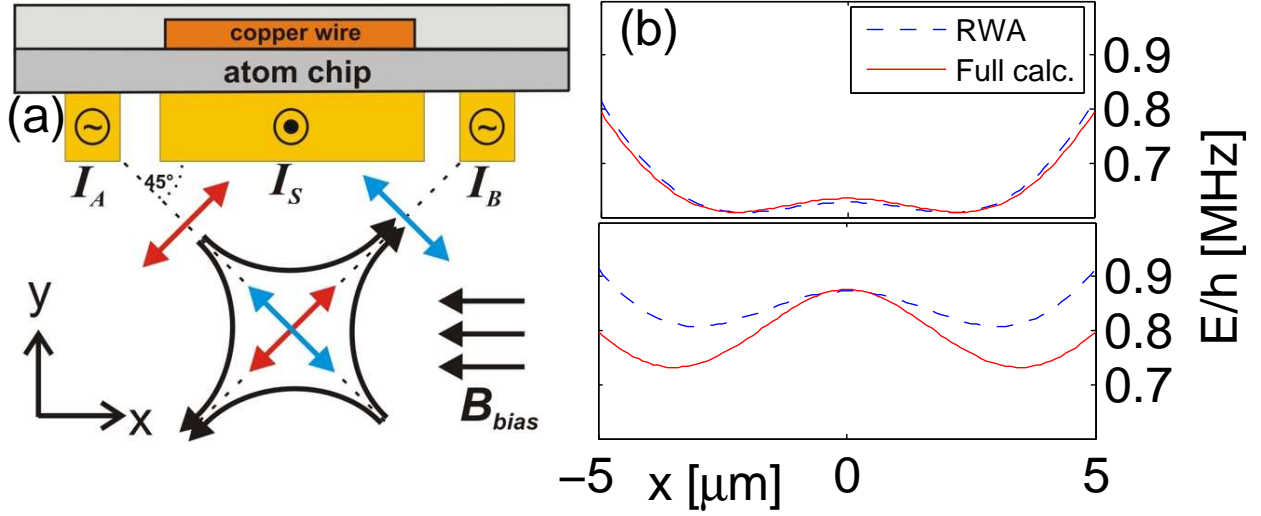


FIG. 1: (a) Schematic of the experimental setup. The central wire creates a static magnetic trap. AC currents of 5...70 mA are applied to the outer wires, which results in dressing fields on the order of 0.1...1.2 G at the trap center. (b) Comparison of potentials obtained using the RWA (dashed lines) and the full calculation (solid line) for two different strengths of the dressing field ($I_{RF} = I_A = I_B = 50$ and 70 mA).

with effective quantum numbers \tilde{m}_F . We will use this notation also to label the dressed states obtained from the full calculation.

To experimentally realize the RF potentials we use a three wire atom chip setup as shown in Fig. 1a. We prepare Bose-Einstein condensates (BECs) of $\sim 10^4$ ^{87}Rb atoms in the $|F = 2, m_F = 2\rangle$ state in a standard Z-wire Ioffe-Pritchard micro trap formed by a DC current in the central wire and a homogeneous bias field [15]. Our scheme of producing BEC in this trap is described in [16]. To create the RF dressing field, AC currents with frequency ω_{RF} and amplitudes I_A and I_B are applied to two additional wires on the atom chip, one on each side of the Z-shaped wire (Fig. 1a). The total dressing field reads $[\mathbf{B}_A(\mathbf{r}) + \mathbf{B}_B(\mathbf{r})e^{i\delta}]e^{i\omega_{RF}t}$, where δ is the phase shift between the two RF currents. This field configuration allows the realization of versatile RF potentials, for example a rotated double well or a ring shaped trap [7, 12].

In the experiments described here, the two RF currents are always equal $I_A = I_B = I_{RF}$, while the phase shift is set to $\delta = \pi$ and the frequency to $\omega_{RF} = 2\pi \times 600$ kHz. The parameters of the static trap are chosen such that $\omega_{\perp} = 2\pi \times 3$ kHz and $\omega_{\parallel} = 2\pi \times 20$ Hz.

The trap center is positioned $115\text{ }\mu\text{m}$ away from the chip surface. The Lamor frequency of the trapped atoms at the trap minimum is $\omega_L = 2\pi \times 650\text{ kHz}$, so that the minimal detuning is 50 kHz . The resulting dressed potential is a symmetric, horizontal double well, with the well separation and the barrier height being controlled by I_{RF} (Fig. 1b).

To calculate the beyond-RWA dressed RF potential of this configuration, we insert the static magnetic field \mathbf{B}_S of the Z-wire trap and the complex amplitude $\mathbf{B}_{\text{RF}}(\mathbf{r}) = \mathbf{B}_A(\mathbf{r}) + e^{i\delta}\mathbf{B}_B(\mathbf{r})$ of the combined RF fields into the Hamiltonian (1) and perform the diagonalization. We observe that although qualitatively the potentials are similar, both the splitting distance and the barrier height are modified quantitatively (Fig. 1b). The latter is changed by more than a factor two for the largest RF dressing fields we have studied. This is of importance for current RF double well experiments, since the tunneling rate between the wells depends exponentially on the potential barrier [17].

Fig. 2a shows the dressed state level structure for an RF current of $I_{\text{RF}} = 60\text{ mA}$. Five levels, which are associated with a single κ and quantum numbers $\tilde{m}_{\text{RF}} = -2, \dots, 2$ are highlighted. It can be seen that different manifolds completely overlap, making a clear separation impossible.

Experimentally, measuring the changes of the well separation and the potential barrier precisely is difficult. The well separation has to be inferred from interference patterns, which is complicated by atom-atom interaction during the expansion of the interfering BECs [6]. The potential barrier could be measured by observing tunneling between the wells [18], but simultaneously reaching a strong RF coupling and an appreciable tunneling rate is again difficult. Instead, we investigate the modification of the RF dressed states due to the beyond-RWA contributions by performing a spectroscopic measurement [10]. We measure the energy difference between dressed states by irradiating the dressed BEC with an additional weak RF "tickling" field $\mathbf{B}_{\text{spec}}(\mathbf{r})e^{i\omega_{\text{spec}}t}$ [14]. If this field is resonant with the dressed state level spacing, transitions to untrapped states are induced. This results in trap loss, which is the signature for a resonance.

We calculate the allowed transitions using time-dependent perturbation theory, writing the operator of the spectroscopy field as $\mathbf{B}_{\text{spec}}(\mathbf{r}) \cdot \mathbf{F}$. This approach is valid only if the spectroscopy field does not deform the dressed states. In our experiments, we use $B_{\text{spec}} \approx 10^{-3} \times B_{\text{RF}}$. We verified experimentally that this treatment is justified by repeating our spectroscopy measurements with a doubled amplitude B_{spec} and observed no measurable

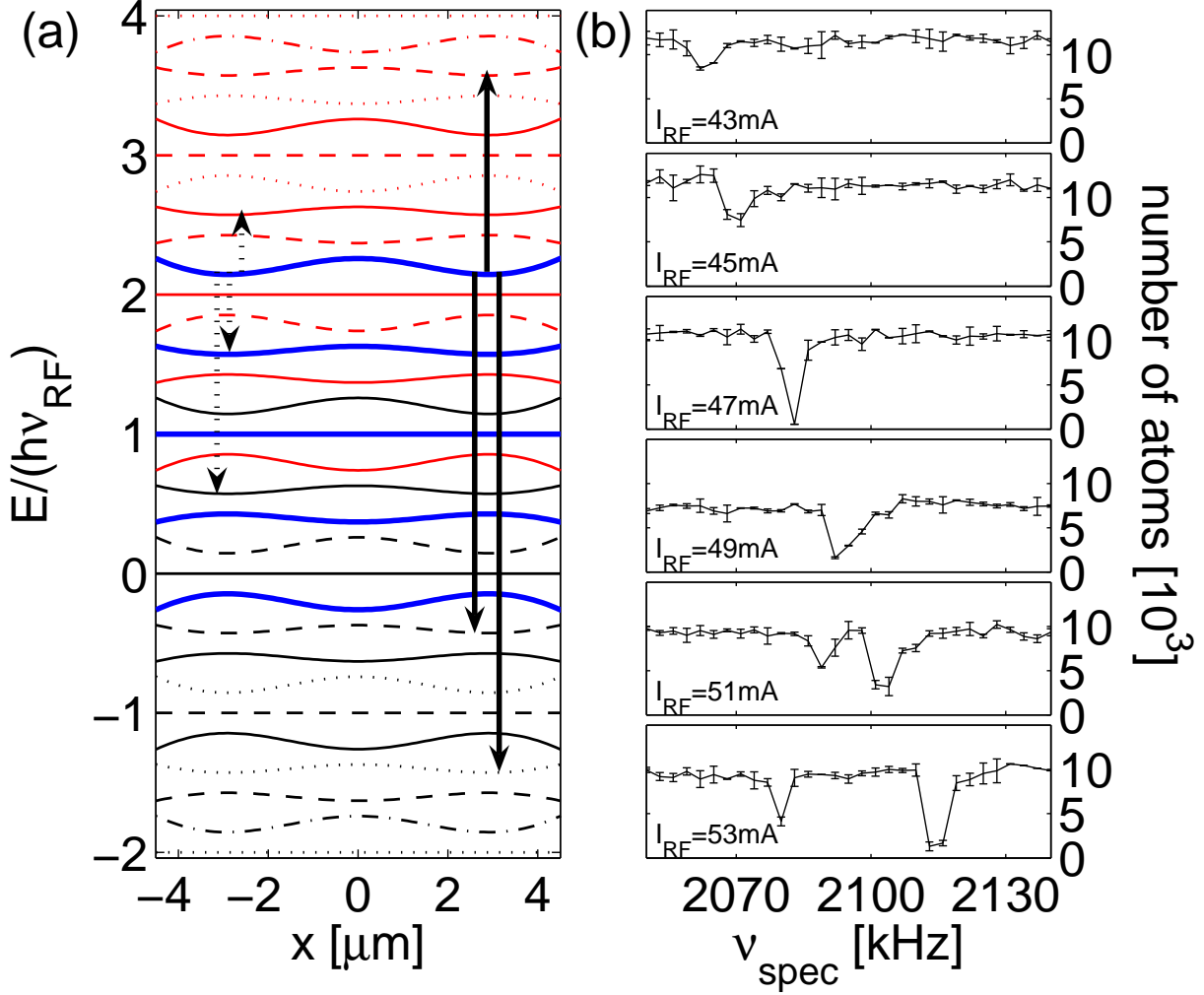


FIG. 2: (a) Level scheme of the RF dressed state potentials for $I_{\text{RF}} = 60$ mA. Five levels associated with one κ -manifold are shown in bold lines. Different manifolds (indicated by color and linestyle) completely overlap for this coupling strength. The arrows mark the transitions induced by the "tickling" field, with the dashed arrows indicating those predicted by the RWA calculation. The full calculation leads to additional allowed transitions (solid arrows). (b) Frequency scans for increasing I_{RF} . The signature of a transition is the loss of atoms from the trap. The strength and the position of the resonances changes with the RF current.

difference in the transition frequencies.

When calculating the transition matrix, we observe that non-vanishing elements only occur if $|\tilde{m}'_{\text{F}} - \tilde{m}_{\text{F}}| = 0, 1$. This means, that although the dressed states are superpositions of all involved bare states, a selection rule similar to the case of RF-transitions between

undressed states exists. This differs for example from spontaneous decay in optical dressing, where transitions between all dressed states can occur [19].

If the RWA is applied to calculate the dressed states, only transitions with $|\kappa' - \kappa| = 0, 1$ occur, resulting in a total of three allowed transitions (dashed arrows in Fig. 2a). This is due to the fact that the RWA dressed states only contain contributions from bare states of a single κ -manifold and that the spectroscopy operator does not act on the photon quantum number of the bare states. In contrast, the full numerical calculation predicts higher order transitions to occur. This is because bare states with different κ contribute to each dressed state. This leads to a chain of allowed transition frequencies given by $\nu_{\text{trans}} = n\omega_{\text{RF}}/(2\pi) \pm \Omega$, where $n = 0, 1, 2, \dots$ and Ω is the energy difference between dressed states within one κ -manifold (solid arrows in Fig. 2a). The calculated transition rates strongly depend on the amplitude of the dressing field. For increasing RF coupling, the higher order transitions become stronger. Additionally, the maximum transition rate is no longer located at $n = 0$ but at higher n . For our parameters, at $I_{\text{RF}} = 60$ mA the $n = 2$ transition is strongest.

The experimental procedure for performing the spectroscopy is as follows: After transferring a BEC from the static trap into the RF potential, we switch on the weak spectroscopy field for a time $t_{\text{spec}} = 100$ ms at frequency ν_{spec} , while all other parameters are held constant. A macroscopic wire 1.2 mm below the atom chip is used to apply this field (Fig. 1a). After the spectroscopy time we switch off all fields and measure the number of atoms by taking a time-of-flight absorption image of the released cloud. Between experiment cycles we vary ν_{spec} and search for frequencies at which we observe atom loss.

Figure 2b shows such scans for different RF currents at frequencies corresponding to the crossing of the $3 \times \omega_{\text{RF}}/(2\pi) + \Omega$ and the $4 \times \omega_{\text{RF}}/(2\pi) - \Omega$ non-RWA transitions. It can be seen that the $4 \times \omega_{\text{RF}}/(2\pi) - \Omega$ resonance only becomes strong enough to cause measurable loss of atoms for large RF currents. The observed transition rates are in good agreement with our numerical results.

In the exact determination of the resonance frequency and the comparison to calculations, the finite temperature and extension of the BEC and its gravitational sag in the potential have to be considered. Taking all errors into account we can determine ν_{trans} with an accuracy of ~ 1 kHz.

The RF spectroscopy can also be used for evaporative cooling in the RF potentials, by sweeping ν_{trans} above a resonance [7, 20]. We have efficiently cooled thermal ensembles to

degeneracy using various RWA and non-RWA transitions. Additionally, we have selectively evaporated atoms from one side of an asymmetric double well.

In Fig. 3 the result of a complete spectroscopy scan between 0 and 2.2 MHz for RF currents $I_{\text{RF}} = 0 \dots 55$ mA is shown. In this scan the appearance of beyond-RWA effects for strong coupling fields can be seen. For low RF currents (small dressing field) we observe three transition frequencies, as predicted within the RWA. The non-RWA transitions are too weak to remove atoms from the trap in the spectroscopy time. The measured transition frequencies are in good agreement with those obtained by the RWA calculation, as can be seen in Fig. 3b. For larger amplitudes of the dressing field, we observe additional transitions at higher frequencies, as predicted by the full calculation.

Furthermore, we observe a shift of the transition frequencies from the RWA calculations (Fig. 3c), which is also in excellent agreement with the full calculation. For the strongest coupling realized, this shift is on the order of 10 kHz, which is one order of magnitude larger than the precision of our measurement. We verify that this effect is indeed a beyond-RWA effect and cannot be ascribed to an uncertainty of our experiment parameters. To this end we independently fit the RWA model to the data, using the field amplitudes as free parameters. This model fails to reproduce the shift of the resonance crossing while at the same time yielding good agreement with the observed resonances for small RF currents. It has to be emphasized that we measure the shift on the energy difference between two dressed states, the absolute deviation between RWA and full calculation for individual dressed states is larger (Figure 1b).

In conclusion, we have shown that RF dressed atoms in an atom chip trap are an ideally suited model system for studying effects beyond the RWA. It allows to access both regimes in which the RWA breaks down, the realization of large coupling as well as (locally) large detuning compared to the resonance frequency. We found that in recent atom chip interference experiments [6, 7, 8] the RF coupling can get strong enough for beyond-RWA effects to become significant. A full calculation of the coupling becomes necessary for an accurate description of the adiabatic RF potentials. We experimentally verified the modifications beyond the RWA by carrying out an RF spectroscopy of a dressed BEC. We find that, beyond the transitions obtained in the RWA, additional higher order transitions occur, as predicted by a full calculation. The observed transition frequencies are in excellent agreement with the numerical results, while there is a clear deviation from the RWA. An

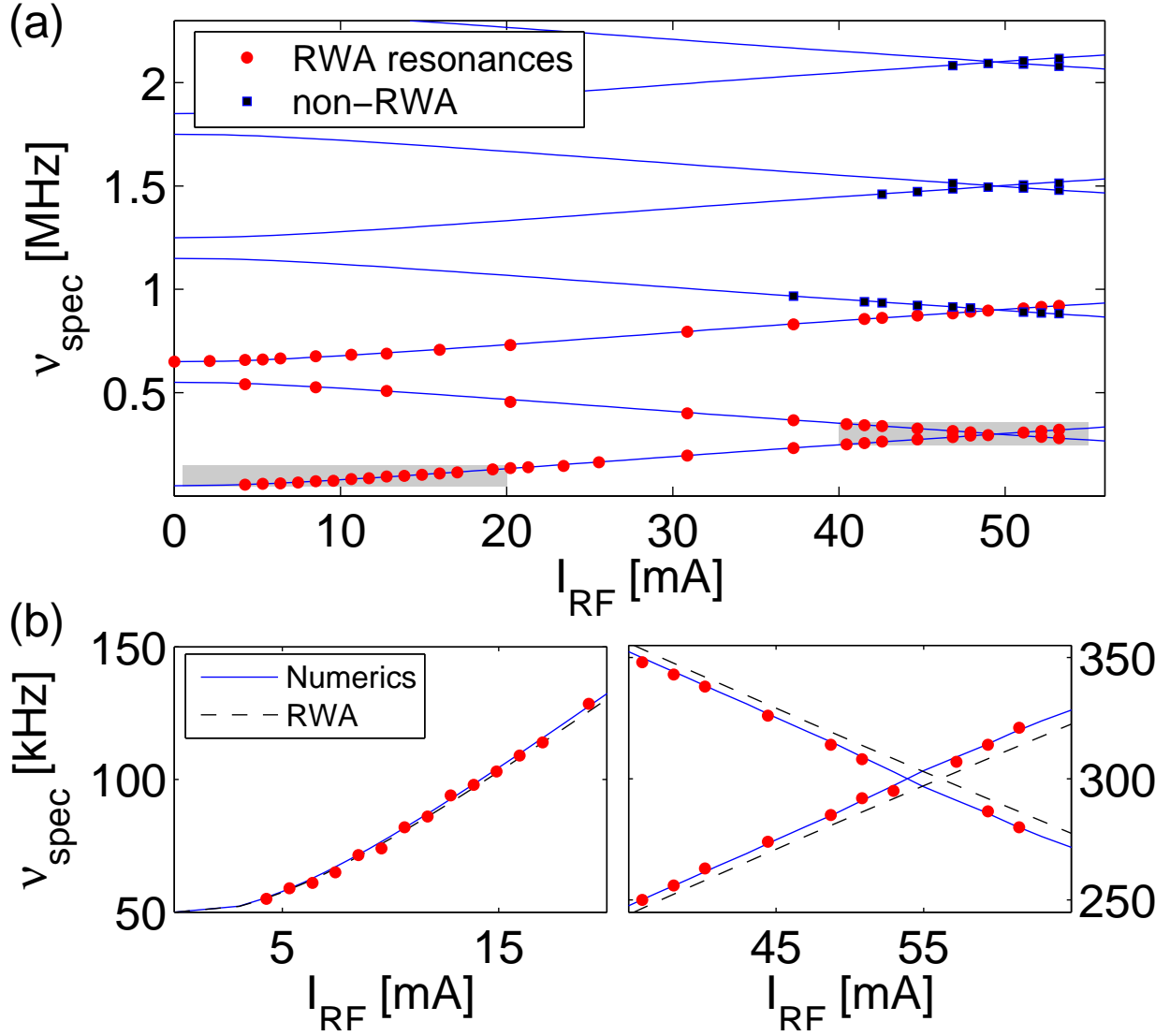


FIG. 3: (a) Observed resonances between 0...2.2 MHz for $I_{\text{RF}} = 0...55$ mA. The numerically calculated transition frequencies are shown as blue lines. It can be seen that for low I_{RF} only three transitions are observable (red points). For higher RF currents additional resonances appear (blue squares). (b) Zoom ins into the two grey-shaded regions of plot (a). Both the numerically calculated transition frequencies (solid line) as well as those obtained from the RWA calculations are plotted (dashed line). For low RF amplitudes the RWA is in good agreement with the full calculation and both agree well with our measurements (left). At higher RF amplitude the non-RWA terms lead to a shift of the resonances which can be measured by the RF spectroscopy (right).

improved accurate knowledge of the adiabatic potentials is very important in current experiments employing RF induced double well potentials, especially for the inferred tunnelling rates. Additionally the RF "tickling" field can be used for efficient evaporative cooling of RF dressed atoms, greatly enhancing the flexibility of RF potentials, allowing for example the study of coherence properties of independently created BECs [7].

We thank J.H. Thywissen for fruitful discussions. We acknowledge financial support from the European Union, through the contracts MRTN-CT-2003-505032 (Atom Chips), Integrated Project FET/QIPC 'SCALA'. I.L. acknowledges support from the European Community and its 6th Community Frame (program of Scholarships of Distinction 'Marie Curie').

* Electronic address: hofferberth@atomchip.org

† Electronic address: igor@iesl.forth.gr

- [1] C. Cohen-Tannoudji, J. Dupont-Roc, and G. Grynberg, *Atom-Photon Interactions* (Wiley, New York, 1992).
- [2] S. H. Autler and C. H. Townes, Phys. Rev. **100**, 703 (1955).
- [3] S. E. Harris, Phys. Today **50**, 37 (1997).
- [4] M. D. Lukin, Rev. Mod. Phys **75**, 457 (2003).
- [5] R. Grimm, M. Weidemüller, and Y. B. Ovchinnikov, Adv. At. Mol. Opt. Phys. **42**, 95 (2000).
- [6] T. Schumm, S. Hofferberth, L. M. Andersson, S. Wildermuth, S. Groth, I. Bar-Joseph, J. Schmiedmayer, and P. Krüger, Nature Phys. **1**, 57 (2005).
- [7] S. Hofferberth, I. Lesanovsky, B. Fischer, J. Verdu, and J. Schmiedmayer, Nature Phys. **2**, 710 (2006).
- [8] G.-B. Jo, Y. Shin, S. Will, T. A. Pasquini, M. Saba, W. Ketterle, D. E. Pritchard, M. Vengalattore, and M. Prentiss, Arxiv **cond-mat/0608585** (2006).
- [9] V. E. Lembessis and D. Ellinas, J. Opt. B: Quantum Semiclass. Opt. **7**, 319322 (2005).
- [10] A. G. Martin, K. Helmerson, V. S. Bagnato, G. P. Lafyatis, and D. E. Pritchard, Phys. Rev. Lett. **61**, 2431 (1988).
- [11] O. Zobay and B. M. Garraway, Phys. Rev. Lett. **86**, 1195 (2001).
- [12] I. Lesanovsky, T. Schumm, S. Hofferberth, L. M. Andersson, P. Krüger, and J. Schmiedmayer,

- Phys. Rev. A **73**, 033619 (2006).
- [13] I. Lesanovsky, S. Hofferberth, J. Schmiedmayer, and P. Schmelcher, Phys. Rev. A. **74**, 033619 (2006).
 - [14] M. Allegrini and E. Arimondo, J. Phys. B: At. Mol. Phys. **4**, 1008 (1971).
 - [15] R. Folman, P. Krüger, J. Schmiedmayer, J. Denschlag, and C. Henkel, Adv. At. Mol. Opt. Phys. **48**, 263 (2002).
 - [16] S. Wildermuth, P. Krüger, C. Becker, M. Brajdic, S. Haupt, A. Kasper, R. Folman, and J. Schmiedmayer, Phys. Rev. A **69**, 030901(R) (2004).
 - [17] A. Smerzi, S. Fantoni, S. Giovanazzi, and S. R. Shenoy, Phys. Rev. Lett. **79**, 4950 (1997).
 - [18] M. Albiez, R. Gati, J. Fölling, S. Hunsmann, M. Cristiani, and M. K. Oberthaler, Phys. Rev. Lett. **95**, 010402 (2005).
 - [19] B. R. Mollow, Phys. Rev. **188**, 1969 (1969).
 - [20] C. L. Garrido Alzar, H. Perrin, B. M. Garraway, and V. Lorent, Phys. Rev. A **74**, 053413 (2006).